Robotics for Systems Integration in Buildings - Pilot Study of Viable Approaches to Install Hygrothermal and Rigid Electrical Systems

Preprint

Naveen Kumar Muthumanickam,[1] Luke Boyd,[2] and Shanti Pless[1]

1 National Renewable Energy Laboratory
2 Colorado School of Mines

Presented at the American Society of Civil Engineers (ASCE) Earth and Space Conference
Miami, Florida
April 15-18, 2024

NREL is a national laboratory of the U.S. Department of Energy
Office of Energy Efficiency & Renewable Energy
Operated by the Alliance for Sustainable Energy, LLC

This report is available at no cost from the National Renewable Energy Laboratory (NREL) at www.nrel.gov/publications.

Contract No. DE-AC36-08GO28308

Conference Paper
NREL/CP-5500-88234
May 2024

Robotics for Systems Integration in Buildings - Pilot Study of Viable Approaches to Install Hygrothermal and Rigid Electrical Systems

Preprint

Naveen Kumar Muthumanickam,[1] Luke Boyd,[2] and Shanti Pless[1]

1 National Renewable Energy Laboratory
2 Colorado School of Mines

Suggested Citation
Muthumanickam, Naveen Kumar, Luke Boyd, and Shanti Pless. 2024. *Robotics for Systems Integration in Buildings - Pilot Study of Viable Approaches to Install Hygrothermal and Rigid Electrical Systems: Preprint*. Golden, CO: National Renewable Energy Laboratory. NREL/CP-5500-88234.
https://www.nrel.gov/docs/fy24osti/88234.pdf.

NREL is a national laboratory of the U.S. Department of Energy
Office of Energy Efficiency & Renewable Energy
Operated by the Alliance for Sustainable Energy, LLC

This report is available at no cost from the National Renewable Energy Laboratory (NREL) at www.nrel.gov/publications.

Contract No. DE-AC36-08GO28308

Conference Paper
NREL/CP-5500-88234
May 2024

National Renewable Energy Laboratory
15013 Denver West Parkway
Golden, CO 80401
303-275-3000 • www.nrel.gov

NOTICE

This work was authored [in part] by the National Renewable Energy Laboratory, operated by Alliance for Sustainable Energy, LLC, for the U.S. Department of Energy (DOE) under Contract No. DE-AC36-08GO28308. Funding provided by the Department of Energy's Advanced Materials and Manufacturing Technologies Office. The views expressed herein do not necessarily represent the views of the DOE or the U.S. Government. The U.S. Government retains and the publisher, by accepting the article for publication, acknowledges that the U.S. Government retains a nonexclusive, paid-up, irrevocable, worldwide license to publish or reproduce the published form of this work, or allow others to do so, for U.S. Government purposes.

Cover Photos by Dennis Schroeder: (clockwise, left to right) NREL 51934, NREL 45897, NREL 42160, NREL 45891, NREL 48097, NREL 46526.

Robotics For Systems Integration In Buildings – Pilot Study of Viable Approaches To Install Hygrothermal And Rigid Electrical Systems

Naveen Kumar Muthumanickam,[1] Luke Boyd,[2] and Shanti Pless[3]

[1] National Renewable Energy Laboratory, Golden, Colorado. Corresponding email: naveenkumar.muthumanickam@nrel.gov

[2] Department of Mechanical Engineering, Colorado School of Mines, Golden, Colorado

[3] National Renewable Energy Laboratory, Golden, Colorado

ABSTRACT

The Industrialized Construction Innovation (ICI) team at the National Renewable Energy Laboratory (NREL) has been exploring the use of robotics to integrate hygrothermal, mechanical, electrical, and plumbing systems in prefabricated building assemblies (offsite construction) and 3D Printed buildings (onsite construction). Such multi-system integration tasks often require specialized robots and custom end-effectors for handling a range of rigid and non-rigid building components. This paper begins with a brief overview of the current state of robotics in construction, followed by a pilot study exploring the use of robotics to integrate a simple prototype multi-trade wall assembly composed of structural studs, hygrothermal layer, wall finishing, and electrical fixtures. The study was funded by the Department of Energy's (DOE) Advanced Materials and Manufacturing Technologies Office (AMMTO). Insights about the implementation of design for manufacturing and assembly (DfMA) principles in designing the prototype wall for robotic assembly, and selection of appropriate robotic end effector hardware for handling these components are included. Detailed comparison of computational toolpath simulations of the robotic assembly process and real-life demonstration of the same is presented. Finally, limitations and lessons learned from this study along with future research recommendations for robotic assembly of more complex multi-trade assemblies, including potential scenarios such as robotic outfitting of facilities in extra-terrestrial environments is included.

Keywords: Building Systems, Design for Manufacturing and Assembly (DfMA), Robotic Assembly, Toolpath Simulation, Advanced Manufacturing, Prefabrication

1. INTRODUCTION

Over the past two decades, robotic technologies have been increasingly adopted by the construction sector for a range of tasks such as excavation, demolition, site surveying, layout marking, brick laying, panelized component installation, and additive construction (or 3D printing) of cementitious walls (Bock, 2007; Gharbia et al., 2020; Melenbrink et al., 2020; Pan et al., 2020; Bademosi et al., 2021; Gusmao et al., 2022; Xiao et al., 2022; Tehrani et al., 2023). Few of these technologies, like additive construction, have matured to achieve high Technology Readiness Levels (TRL), leading to multiple single story and multi-story buildings 3D Printed using several region specific 3D Printable concrete or cementitious mixes across continents (3Dnatives, 2021; 3DPrintingIndustry, 2023; NPR, 2023). There are even conceptual demonstrations showcasing the potential of utilizing robotic additive construction to construct extraterrestrial habitats and

infrastructure on the Moon and Mars (Muthumanickam et al., 2020, 2021a). While robotic solutions for constructing walls and structural components (marked in red in Figure 1) are maturing rapidly, robotic solutions for integration of other systems and components in buildings (Figure 1) are still in their infancy.

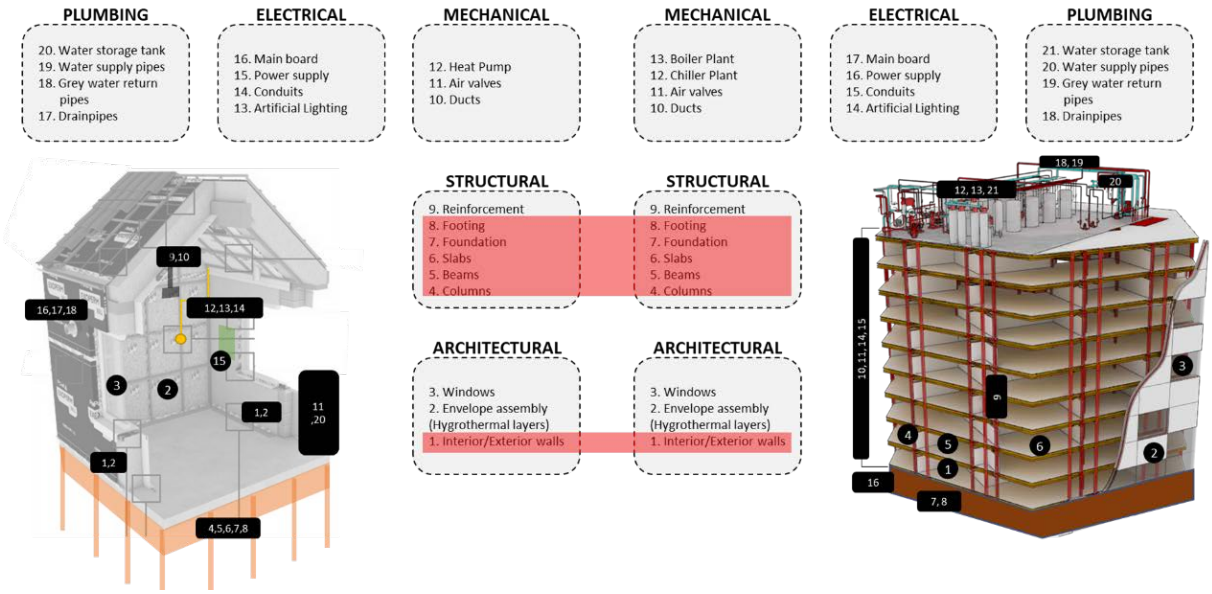

Figure 1: [Left] Various systems in residential and [Right] commercial buildings where robotic construction developments predominantly focus on highlighted systems (Adapted from Muthumanickam et al., 2021).

Optimal integration of these other systems like hygrothermal control layers for optimal envelope shielding from outdoor environmental conditions, mechanical, electrical, and plumbing (MEP) components for heating, ventilation and air conditioning (HVAC), and fire protection, are crucial for the effective functioning of buildings (Muthumanickam, 2021b). Even more, modern buildings include additional components for power generation (building integrated photovoltaic panels), storage (batteries), specialized power distribution systems (charging outlets) and control systems. Advancements like offsite factory based prefabrication of building system assemblies including panelized, and volumetric modular construction have gained significant market traction for rapid integration of these systems across the residential, commercial, hospitality, healthcare, pharmaceutical, manufacturing, and datacenter construction sectors. Nevertheless, the majority of such offsite construction factories demonstrate limited to infrequent use of robotics, thereby constraining the complete productivity advantages of a controlled production environment. The Industrialized Construction Innovation (ICI) team at NREL is developing robotic solutions for integrating these systems and components in offsite and onsite construction at scale and speed without compromising on quality control. These include telerobotic, semi-autonomous and autonomous modes of operation appropriate for the task at hand.

While preliminary studies indicate robotics for integrating such multi-trade systems warrants a range of DfMA principles and customized robotic end-effector for different components, this paper exclusively focuses on dissecting the robotic integration of a prototype wall assembly consisting of structural studs, insulation, electrical raceway and outlet. A comprehensive overview of the DfMA of the various components of the prototype wall assembly, programming of robotic

equipment to assemble the components, design and fabrication optimization for mitigating robotic constructability constraints are covered in Section 2, followed by the limitations of the study in Section 3. This study aims to act as a precursor for future investigations into the utilization of robotics for systems integration in buildings on a broader scale, encompassing more complex multi-trade building systems. It is noteworthy that the National Aeronautics and Space Administration (NASA) is invested in the research and development of robotic solutions for outfitting Lunar infrastructures like pressurized habitats, power generation towers, launch and landing pads, with various systems and components for power generation, storage, distribution, air filtration and distribution, and other relevant utilities to ensure proper functionality. Consequently, Section 3 also includes a brief discussion on extrapolating the inferences from this research to lend itself to potential use-cases such as robotic outfitting of extra-terrestrial facilities.

2. PILOT STUDY – ROBOTIC WALL SYSTEM ASSEMBLY

2.1. Design for Manufacturing and Assembly (Wall and Robotic Equipment)

Typically, building walls are composed of wood, steel, or concrete framing for structural integrity; foam, cellulose, mineral wool, fiberglass or aerogel insulations for heat transfer management; air, water, and vapor barriers for infiltration control; glass windows for heat, light and ventilation management; gypsum board, wooden panels, metal panels, tiles, concrete, or bricks for interior and exterior finishing; air ducts, electrical conduits, and pipes for MEP distribution; and grills/vents, power outlets, switches, faucets, and shower heads, for controlling MEP systems. For the sake of the pilot study, the prototype wall assembly was designed after a typical residential construction wall system consisting wooden studs, rigid foam board insulation, electrical outlet, raceway and interior and exterior plywood panel finishing. Typically, drywall (gypsum boards) is used as finishing material, however, plywood was selected for two reasons namely a) fragility of gypsum boards for robotic handling and b) logistical constraints of handling gypsum in indoor environments at NREL. Since the pilot study exclusively focused on exploring robotic constructability of the prototype wall assembly, it was essential to consider the specific manufacturability and constructability constraints associated with the deployed fabrication machinery and robotic equipment during the wall assembly design. A 6-axis robotic arm with a payload capacity of ~11 pounds and a reach/sphere of influence of four feet in all directions from the central axis of the robotic arm was used for pilot study. Further, the robotic arm was positioned on a 30 inch tall pedestal for increasing the default maneuverability and reach (Figure 2).

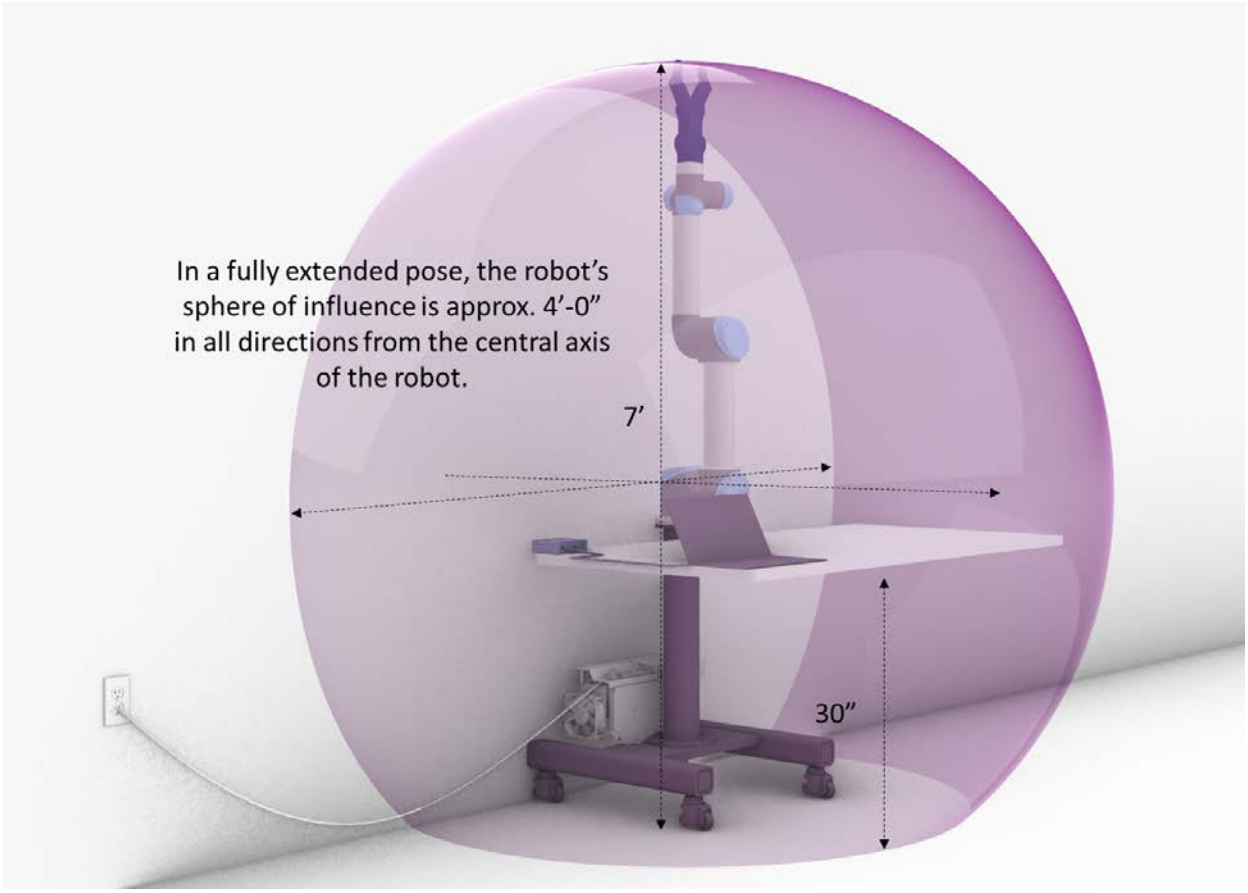

Figure 2: 3D Representation of the sphere of influence of the 6-axis robotic arm setup on a pedestal.

Taking into account the technical constraints of the robotic arm such as payload capacity and reach, the prototype wall assembly was designed as a miniaturized 3' x 3' representation of an actual residential wall. Figure 5 shows 3D representations of the prototype wall assembly modeled in Rhino 3D™. It was designed to have five 2" x 4" studs - bottom stud (#3 in Figure 3), left stud (#4 in Figure 3), right stud (#5 in Figure 3), middle stud (#6 in Figure 3) and top stud (#11 in Figure 3); two pieces of custom cut rigid foam insulation (#9 and #10 in Figure 3); and four pieces of plywood sheets (#12, #13, #14, #15 in Figure 3). The studs were designed with mortise and tenon joints to simulate slide-in joineries as an alternative to nailing, to secure components in place. Since the prototype wall assembly was designed to be robotically assembled in an upright position without anchoring the base stud to the ground, a 4" x 6" piece of lumber with a 1" deep cut out was envisioned to be used as a base piece (#1 in Figure 3) to accommodate and secure the bottom stud in position. The base piece was embedded with six 4" tall Aluminum C-Channels (#2 in Figure 3) for the plywood panels to slide in place as a wall finish. The middle stud was designed to be affixed with an electrical box with 4 *gangable* outlets (#7 in Figure 3) and a raceway (#8 in Figure 3) feeding the same. The raceway is a conduit to contain the wiring that powers the electrical outlets. The scope of this paper does not include the robotic insertion of non-rigid components, such as wires within the raceway, and will be addressed in a future paper.

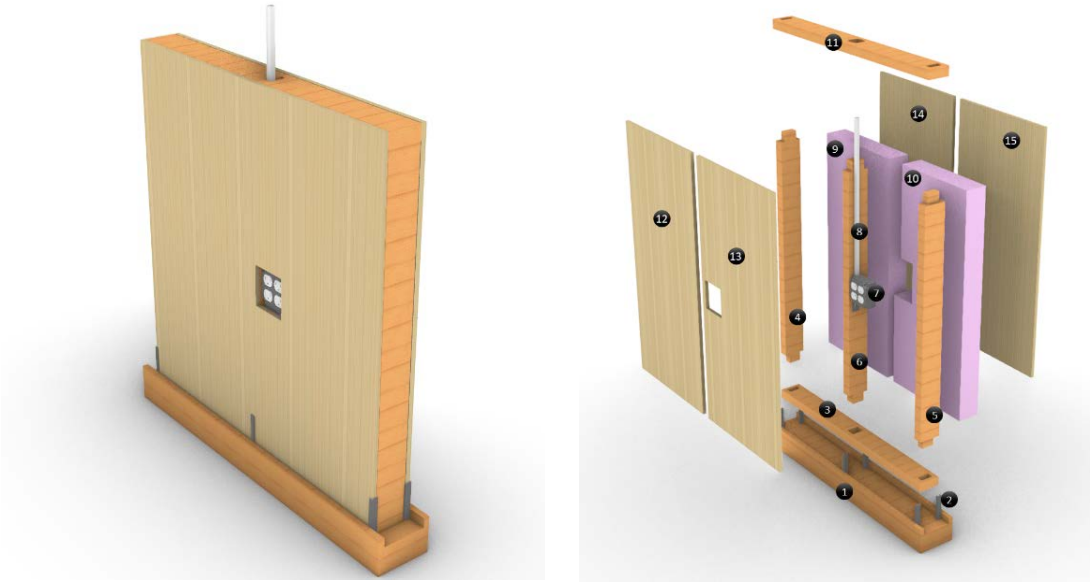

Figure 3: [Left] Render and [Right] Exploded 3D of prototype wall assembly designed for robotic assembly testing.

Further, based on the geometry and physical characteristics of the wall components to be handled, the robotic arm was outfitted with three types of end-effectors, namely a Two-finger Gripper (payload capacity - 4.5 pounds) with an adjustable *stroke* (distance between the two fingers) up to 4.33 inches, an Electric Vacuum Suction Gripper with configurable suction cup arrays (payload capacity - 44 pounds), and a Screwdriver end-effector (torque range of 9 in-pounds to 35 in-pounds) capable of handling #3 to #10 sized metal screws with variable drives (Figure 4).

Figure 4: [Left to Right] Two-finger Gripper, Electric Vacuum Suction Gripper, and Screwdriver end-effector.

2.2. Robot Programming and Virtual Simulation

Subsequently, the robotic setup along with the prototype wall assembly was modelled in Rhino 3D™ for the purpose of virtual simulation and programming of the sequence of robotic assembly tasks as listed in Table 1. Grasshopper™, a node based parametric programming plugin within Rhino 3D™ along with Universal Robots URCaps™ SDK (Universal Robots, 2024) was utilized for writing control algorithms to program the robot and the end-effectors. The algorithm was structured to take the *centroid* coordinates of the various components of the prototype wall assembly at its initial and final positions as input variables and compute an optimal robot toolpath (motion planning) between these two positions. For instance, a_1, c_1, d_1, e_1, f_1, g_1, h_1, i_1, j_1, k_1, l_1 are the centroid coordinates at the initial position and a_2, c_2, d_2, e_2, f_2, g_2, h_2, i_2, j_2, k_2, l_2 are the centroid coordinates at the final position for the respective components in Steps 2, 5, 6, 8, 9, 10, 11, 12, 13, 14, and 15, respectively. The placement of the middle stud was programmed as two

distinct steps (Steps 4 and 7) - initial position b_1 to an intermediate position b_2, and intermediate position b_2 to final position b_3, for collision avoidance based on several simulated iterations. Note that a_{2^1} and a_{2^2}, and a_{2^3} and a_{2^4}, represent the coordinates of two screw holes for each component on the middle stud - specifically, the electrical outlet, and the bracket holding the raceway - when they are in their final position a_2 on the middle stud (at its initial position b_1).

Table 1: Sequence of steps envisioned for robotic assembly of prototype wall assembly

Sequence	Task Description (Tool)
Step 1	Place base piece with six embedded Aluminum C-Channels (Manual)
Step 2	Pick and place electrical outlet + raceway (with mounting brackets) from a_1 to a_2 on middle stud (Two-finger Gripper)
Step 3	Screw electrical outlet + raceway mounting brackets to middle stud at a_{2^1} and a_{2^2} (screw holes in electrical outlet mounting bracket), a_{2^3} and a_{2^4} (screw holes in electrical raceway mounting bracket) (Screwdriver End-Effector)
Step 4	Pick and place middle stud (with integrated electrical outlet + raceway) from b_1 to b_2 (Two-finger Gripper)
Step 5	Pick and place bottom stud from c_1 to c_2 (Two-finger Gripper)
Step 6	Pick and place left stud from d_1 to d_2 (Two-finger Gripper)
Step 7	Pick and place middle stud (with integrated electrical outlet + raceway) from b_2 to b_3 (Two-finger Gripper)
Step 8	Pick and place right stud from e_1 to e_2 (Two-finger Gripper)
Step 9	Pick and place insulation piece 1 from f_1 to f_2 (Electric Vacuum Suction Gripper)
Step 10	Pick and place left insulation piece 2 from g_1 to g_2 (Electric Vacuum Suction Gripper)
Step 11	Pick and place top stud from h_1 to h_2 (Two-finger Gripper)
Step 12	Pick and place plywood panel 1 from i_1 to i_2 (slide into C channel) (Simulated with Two-finger Gripper, executed with Electric vacuum Suction Gripper)
Step 13	Pick and place plywood panel 2 from j_1 to j_2 (slide into C channel) (Simulated with Two-finger Gripper, executed with Electric vacuum Suction Gripper)
Step 14	Pick and place plywood panel 3 from k_1 to k_2 (slide into C channel) (Simulated with Two-finger Gripper, executed with Electric vacuum Suction Gripper)
Step 15	Pick and place plywood panel 4 from l_1 to l_2 (slide into C channel) (Simulated with Two-finger Gripper, executed with Electric vacuum Suction Gripper)

The electrical box and raceway mounting brackets were programmed to be screwed to the middle stud while it was in a horizontal position for easy assembly, to leverage gravity-assisted screwing (Step 3). The screwdriving steps were simulated using a multi-functional robotic screwdriver end effector. Furthermore, as outlined in Table 1, the robot had to be outfitted with three different end effectors for the various steps. The process of changing the end effectors was manual and the robot toolpath (motion plan) was programmed to have *travel moves* (move to an arbitrary *safe change* position away from the prototype) to accommodate such manual tool changes between Steps 2 and 3, 3 and 4, 8 and 9, and 10 and 11, respectively.

The Tool Center Point (TCP) of the robotic end effector used in each step, was programmed to align with the centroid coordinates of the various components, all along the trajectory from their initial to final positions. The stroke (distance between the two fingers of the gripper) of the two finger gripper end effector was programmed to be 4.33 inches during travel moves and release of components at their final position, and be the width (inches) of the components while carrying them from initial to final positions. The gripper was programmed to exert a controlled compressive force of ~8.9 pounds (max limit of hardware) to securely grip the objects while carrying them. Similarly, the electric vacuum suction gripper was programmed to operate at -0.73 psi during travel moves and release of components, and at -11.74 psi while carrying components (rigid foam insulation and plywood panels). By default, the control algorithm programmed using Grasshopper™ and URCaps™ SDK would generate a toolpath (straight red lines passing through multiple objects in left side of Figure 5) that might have multiple collisions with other components, and inverse kinematic errors due to infeasible robot joint angles during the execution. To mitigate this, each component was modelled as a collider within the algorithm, and the reward function was set to incentivize the toolpath with minimal collisions and inverse kinematic errors (right side of Figure 5). This ensured that the resultant toolpath is a combination of optimal joint angles for the robot to carry out a given task (pick and place / screwdriving) efficiently with zero collisions and inverse kinematics errors. Figure 6 showcases the simulated sequence of robotic tasks.

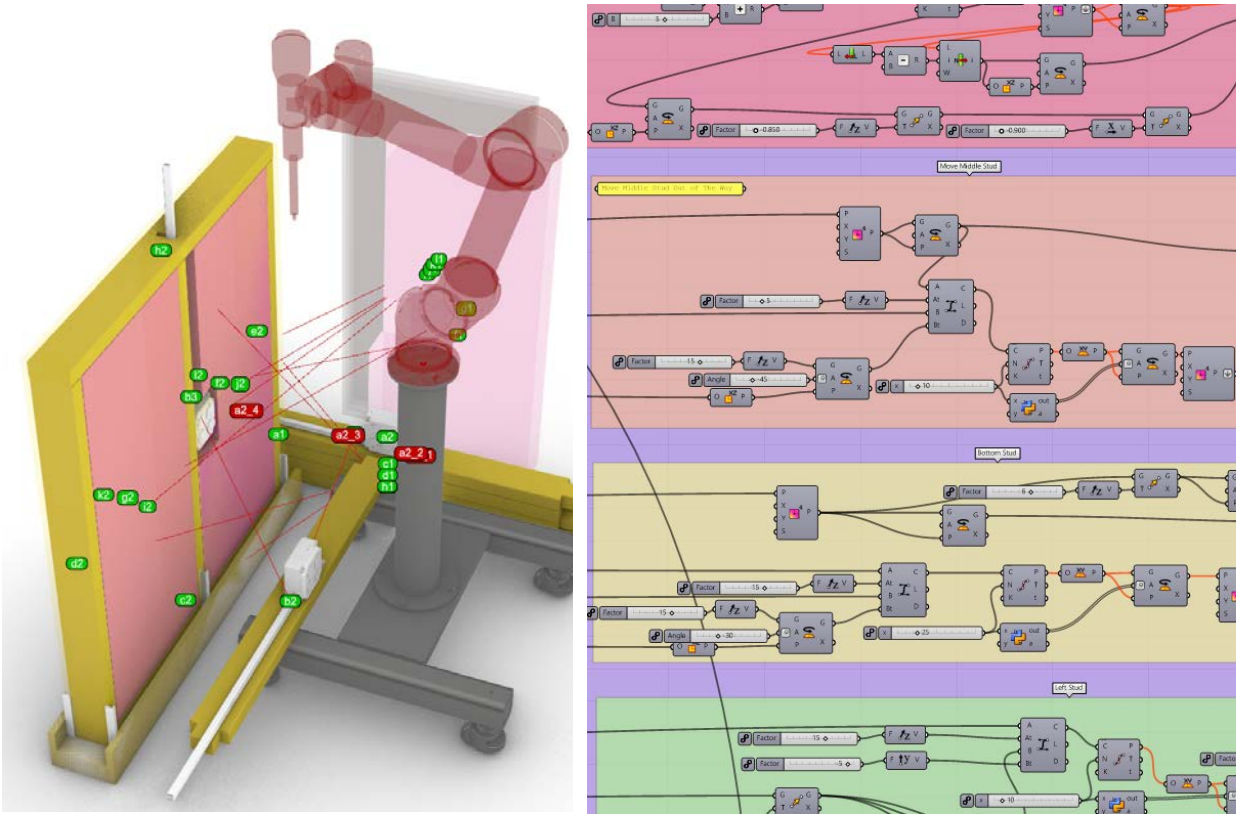

Figure 5: [Left] Snapshot of robotic toolpath with collisions shown as red lines. [Right] Snapshot of part of the algorithm developed for collision free toolpath (motion planning) generation and robot control.

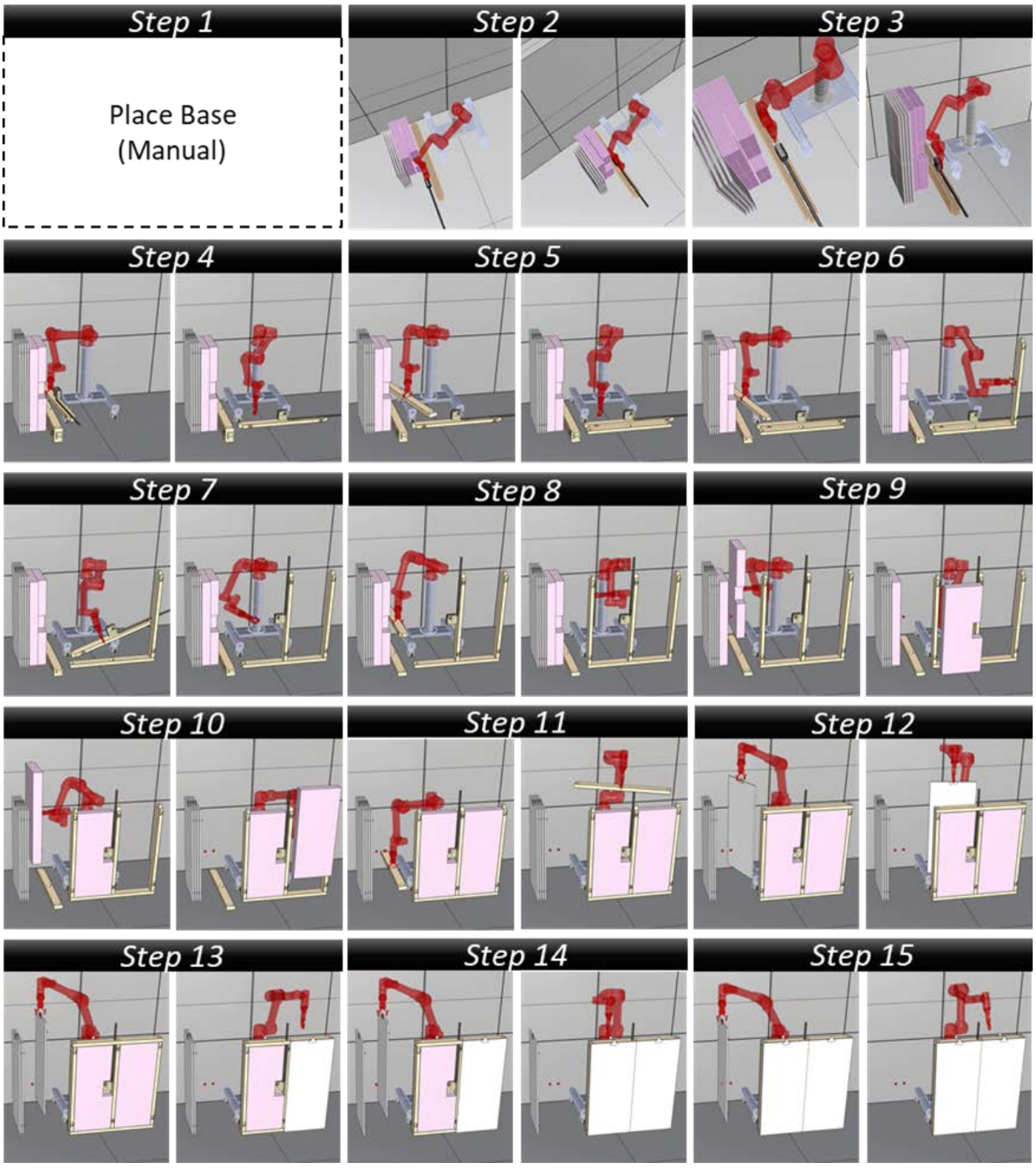

Figure 6: Simulated sequence of tasks in robotic assembly of prototype wall assembly (Base Piece not shown in any step of the virtual simulation).

2.3. Sourcing and Fabrication

After successful simulation and visualization of the toolpaths for the specified sequence of steps involved in the robotic assembly of the prototype wall section, the raw materials for each component were sourced and fabricated into the designed components using the fabrication techniques outlined in Table 2 and Figure 7.

Table 2: Overview of design spec fabrication of various components in prototype wall assembly from appropriate raw materials

	Raw Material Form Factor	Designed Component Form Factor and Name Identifier	Fabrication Technique
1	4”x 6”x 8’ Dimensional Lumber Stud	 Base Piece	-Cut to specific length using Band Saw -Milled to a depth of 1” using Knee Mill to accommodate the bottom stud of wall assembly.
2	2”x 4”x 8’ Pinewood Stud	 Bottom, Left, Right, Middle and Top Studs	-Cut into 5 studs of specific lengths and corner profiles as in picture using Band Saw -Milled holes to accommodate Mortice and Tennon joints using Knee Mill -Attached SS electrical box, raceway channel and triangular base (design change incorporated later for reasons covered in Section 2.4) to middle stud manually
3	1”x 4’x 8’ Rigid Foam Insulation	 Left and Right Insulation	-Cut 6 separate pieces of insulation (3 of each profile type as shown in picture) using Band Saw and glued 3 of each type together to form two 3” thick pieces. Triangular cut at the bottom of one of the insulation pieces was a design change incorporated later for reasons covered in Section 2.4.
4	8’x4’ Plywood Sheet	 Plywood panels 1,2,3, and 4	-Cut into 4 separate pieces of plywood (used in place of drywall in prototype wall assembly) as shown in picture using Band Saw
5	Raceway	 Raceway	-Cut to 24” (later changed to 18” for reasons covered in Section 2.4) using Band Saw
6	Raceway Accessories	 Raceway clamps	-Off the shelf component
7	20 Amp Duplex Stainless Steel Electrical Outlet		-Off the shelf component
8	4 in. 30.3 cu. in. Square Gangable Stainless Steel Switch Box with clamps and CV bracket		-Off the shelf component
9	4” Square Stainless Steel Electrical Box Cover		-Off the shelf component
10	Aluminum C Channel/Scrap Metal		-Six ~4” tall aluminum C channels made of scrap aluminum embedded upright as shown in figure, as a mechanism for the plywood panels to slide in place as a finishing for the wall assembly

Figure 7: [Left to Right] Milling of wood and metal using Knee Mill, 3-axis Knee Mill setup, Aluminum C-Channel Cutting and Drilling

2.4. Robot Programming and Actual Simulation

Once the components for the prototype wall assembly were fabricated to the specification, an actual simulation of each step of the robotic assembly sequence was carried out to identify any anomalies or discrepancies. For safety and observational purposes, the joint speed was reduced to 30 % of the original maximum speed for each joint (Original Speed of joints - Base: ± 180°/Sec. Shoulder: ± 180°/Sec. Elbow: ± 180°/Sec. Wrist 1: ± 360°/Sec Wrist 2: ± 360°/Sec Wrist 3: ± 360°/Sec). Since the prototype wall assembly was a programmed robotic task and not autonomous, the initial positions of the fabricated components in the virtual model had to be replicated in reality with very minimal to no tolerance differences to avoid variations between the virtual simulation and actual setup as shown in Figure 8.

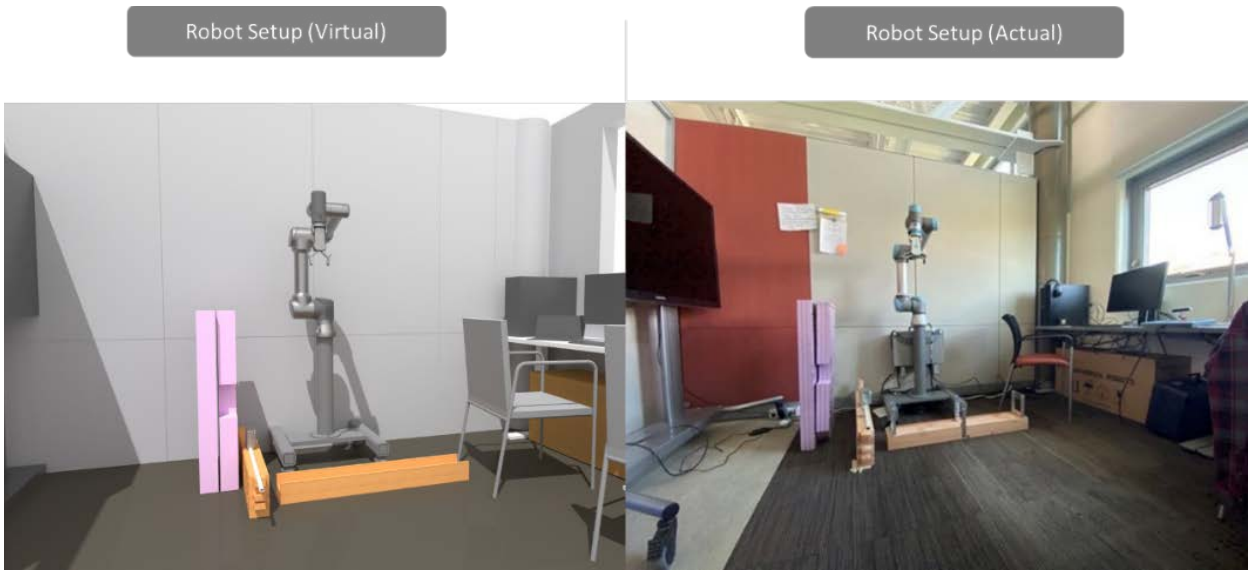

Figure 8: [Left] 3D model of robotic construction setup. [Right] Actual version of robotic construction setup.

Despite matching the actual setup to mimic the virtual model, toolpath simulations that were successful in the virtual model without any collision or inverse kinematic errors failed during actual simulations due to a range of issues pertaining to tolerance, physics, and inverse kinematic solver discrepancies as shown in Figure 9.

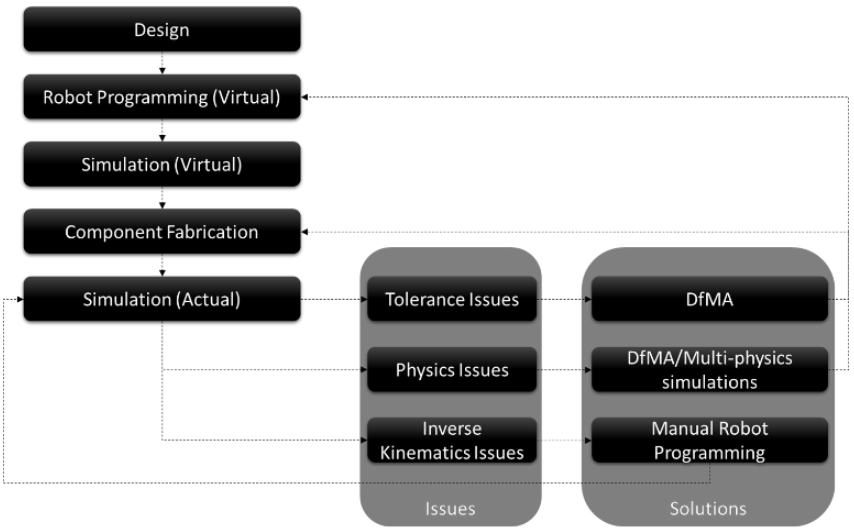

Figure 9: Issues experienced during actual implementation of robotic wall assembly and potential solutions to the issues.

For example, though virtual simulations of Steps 6, 7, and 8 in Table 1 indicate no errors or anomalies, in actual reality the three vertical studs (left, middle, and right stud) did not slide seamlessly between the C-Channels due to friction caused by tolerance errors. Motion planning simulations fail to capture such nuanced object interactions as they don't account for fabrication discrepancies. To address this issue, DfMA strategies like reducing the width of the stud pieces near their interaction point with the C-Channel by shaving some wood using a Knee Mill were explored. This enabled the studs to slide well between the C-Channels as shown in Figure 10.

Figure 10: [Left] Stud without milled sides brushing against Aluminum C-Channel and (Right) Stud with milled sides to seamlessly slide in place between the Aluminum C-Channels

Similarly, after executing Step 7, the middle stud kept leaning towards one side due to the weight of the electrical outlet attached to it. To prevent the leaning, a small triangular buttress was affixed to the bottom of the middle stud. The bottom of one of the insulation pieces had a cutout to accommodate the triangular buttress at the bottom of the middle stud. However, the addition of the triangular buttress to one end of the middle stud, made the stud to have tilted orientation while being carried by the two finder end effector, as opposed to a perfectly horizontal orientation as seen in the virtual simulations (Step 4). This disorientation caused collision concerns with other components during the robotic assembly. To solve this issue, a bolted nut was attached to the middle stud on the side opposite to the triangular piece to act as a counterweight and offset the tilt as shown in Figure 11.

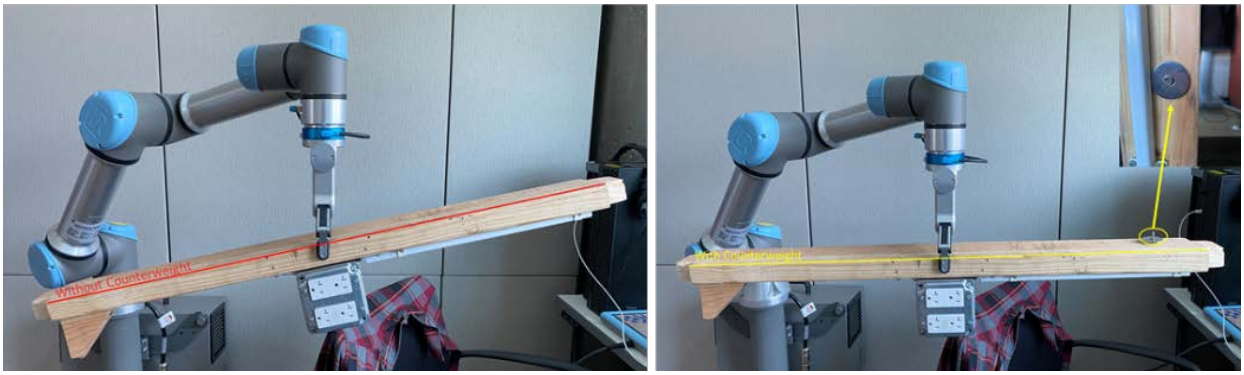

Figure 11: [Left] Middle Stud without counterweight and [Right] with counterweight.

Originally, the plywood panels were programmed to be carried and placed in position using the Two-finger gripper end-effector. However, this mechanism kept failing due to the weak grip by the two finger gripper end-effector on the plywood panels. As an alternative, the plywood panels were programmed to be lifted using the electric vacuum suction gripper similar to the insulation. This also helped avoid the need for props to hold the plywood panels and the insulation pieces upright, as they were stacked flat on top of each other on the ground. However, due to the porosity of the untreated plywood panels, and rigid foam insulation, the vacuum suction gripper sometimes failed in establishing an airtight seal between the cup and the object's surface, which is crucial for generating necessary lifting force. To mitigate this, the plywood panels and insulation pieces were covered with pressure sensitive adhesive tape (cellophane tape) at their point of contact with the vacuum suction gripper (seen in Step 13 of Figure 14). Also, the electric vacuum suction gripper was tested in compact, partially expanded and fully expanded configurations of suction cup arrays to evaluate if maximizing the target area for negative pressure induced surface adsorption resulted in any increase in lifting efficiency (Figure 12). After several iterations, compact and fully expanded configurations were adopted to carry the plywood panels and rigid foam insulation pieces, respectively.

Figure 12: [Left to Right] Compact, partially expanded, and fully expanded configurations of the electric Vacuum Suction Gripper End Effector.

Another issue was that the built-in *inverse kinematic solver* (Aristidou et al., 2009) used in the virtual simulations was partially different from the solver within the onboard processor of the actual 6-axis robotic arm. This led to several joints behaving differently from the virtual simulations leading to partial collisions and singularity points. Such discrepancies were overcome by overriding the virtually simulated toolpath with manual robot programming. The 6-axis robot at our disposal being a COllaborative roBOT (COBOT) had the capability to record robotic trajectories that were manually programmed using the *teach pendant* or hand guided motion of the robot in *freedrive* mode (Universal Robots, 2023). However, the capability to relay this recorded robotic trajectory and end-effector action(s), back into the virtual simulation to integrate it with the whole program was lacking. Hence, the robot control algorithm was modified to enable both

"feed-forward" and "feed-backward" information exchange capabilities between the computer and the robot (Figure 13). This way, real time visualization of both the virtual simulation as well as recorded manual modifications to the robotic trajectories was possible. Figure 14 showcases the snapshots from the sequence of robotic tasks involved in the integration of the prototype wall assembly.

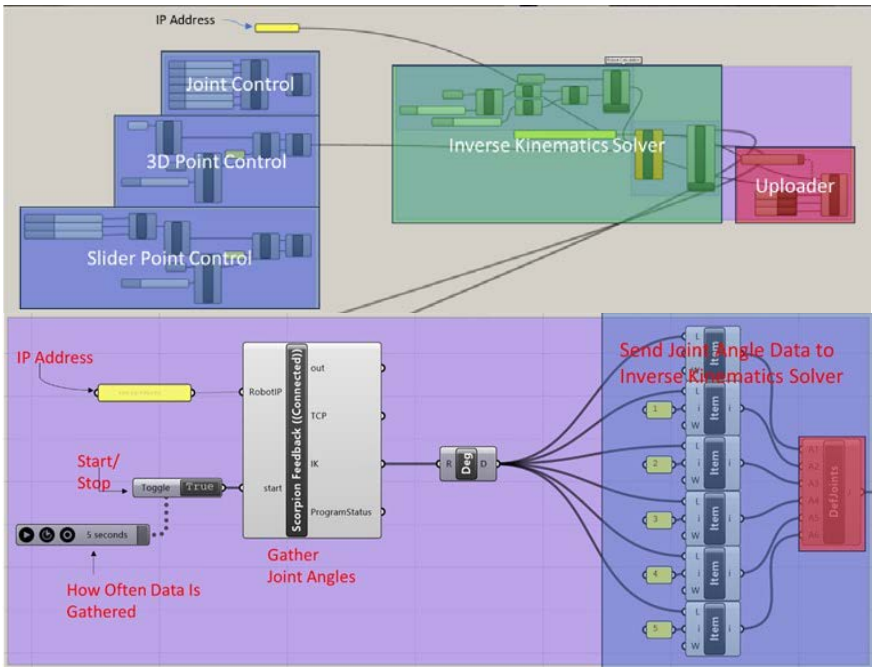

Figure 13: [Top] Grasshopper nodes facilitating "Feed Forward" PC to Robot transmission, [Bottom] Grasshopper nodes facilitating real-time "Feed Backward" Robot to PC transmission.

A steel electrical box with 4 *gangable* outlets (#7 in Figure 3), and a 24" long Aluminum raceway, were attached together as a single piece using a bolt and nut for ease of robotic assembly. Further, this assembly was affixed with three Aluminum brackets - one on the electrical box and two along the length of the raceway, with two screw holes in each bracket. After robotically picking and placing this integrated electrical assembly on top of the middle stud (see Table 1), a screw driver end-effector was used to drive four 1/4" #4 Screws with indented, unslotted hex washer heads to secure the brackets of the electrical outlets and raceway to the middle stud (see Table 1 for positions of screws). Typically, the Screwdriver end-effector collects, via vacuum action, a screw dispensed by an automated Screw Feeder hardware; holds the screw in place during robotic motion towards the target location, positioning and driving processes. However, since the automated Screw Feeder hardware was unusable at the time of this pilot study due to logistical constraints, the screws were manually loaded into the vacuum powered Screwdriver end-effector tip/sleeve, subsequently followed by the robotic screwdriving. To prevent the stud from torque induced rotation during screwing, impromptu manual anchoring methods such as clamping were employed, which were not visually represented in the simulations. Also, the screws were driven directly into the studs without any plugs. To facilitate easy swapping between the three types of end-effectors used in various steps, two types of quick change adapters with a *snap in – snap out* mechanism were explored – one with a single tool holder and another one with a dual tool holder (shown in Step 13 in Figure 14).

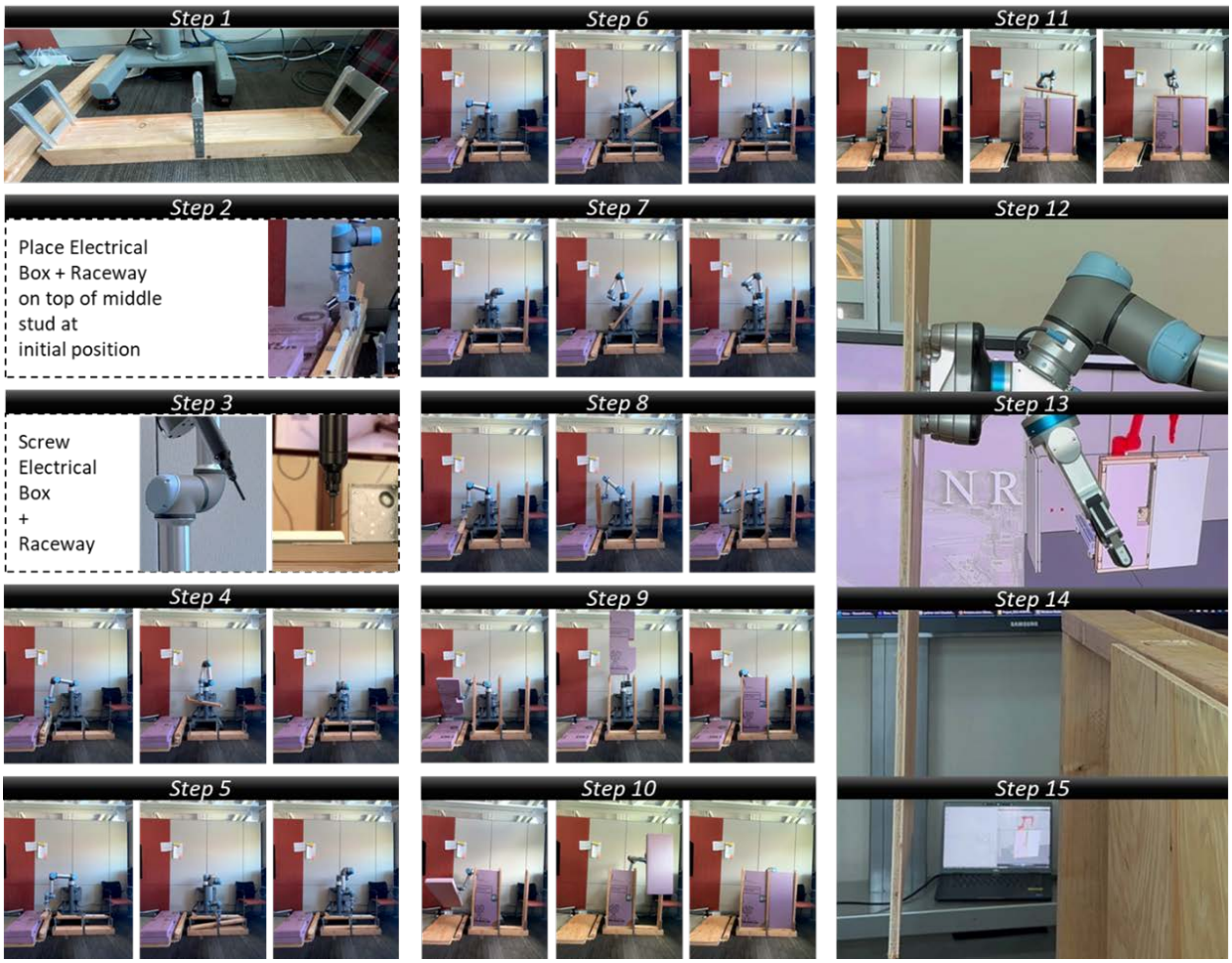

Figure 14: Snapshots from the sequence of robotic tasks involved in the integration of the prototype wall assembly. Dual quick change adapter for easy tool swapping shown in Steps 13-15.

3. LIMITATIONS, LESSONS LEARNED, & RECOMMENDATIONS

The pilot study revealed tolerance, physics, and inverse kinematics issues in robotic assembly of a small-scale prototype made of wood, rigid foam, and metal. Actual buildings, with more complex systems and materials like concrete, steel, aluminum, glass, and polymers, pose additional challenges. Even more advanced use cases like lunar construction, in particular, requires specialized materials, such as sophisticated composites, to manage extreme temperature fluctuations and micrometeoroid impacts. Tighter tolerance and dimensional control are essential for seamless robotic integration in such multi-material assemblies. As highlighted in this pilot study, the success of robotics for systems integration depends equally on the implementation of both DfMA strategies and precision fabrication. While manufacturing industries adhere to strict international standards like ISO 9001 and ISO 14405, providing guidelines for precision in micrometers or nanometers, the construction industry generally operates with larger tolerance measured in millimeters or centimeters. Utilizing advanced manufacturing techniques like Computer Numerical Control (CNC) milling, lathe, routing, plasma cutting, laser cutting, grinding, and welding to prefabricate construction components becomes crucial to achieve the precision tolerance and tight dimensional control appropriate for robotic assembly.

While the study primarily focused on pick and place tasks, potential applications such as rebar placement in 3D printed walls, air duct installation, plumbing, cable routing, glass installation, etc., may require additional robotic fabrication tasks like welding, bending, cutting, and finishing. These scenarios might necessitate larger robots with custom end-effectors featuring increased payload capacity and maneuverability for handling sizable construction components. Despite using quick change adapters in the pilot study (Figure 14), the manual action of swapping end-effectors required programming the robot to travel to a *safe change* location with intermediate stops. An automated tool change mechanism would eliminate these redundancies, enhancing the overall productivity of robotic automation.

As the construction components and robotic systems become more complex in the construction of intricate infrastructure, solely relying on simulations makes it challenging to assess nuanced collisions due to the robot's intricate maneuvers. Further, the orientation of the components during robotic motion in real life situations might sometimes differ from virtual simulations due to their inherent material properties. Virtual simulations that solely evaluate inverse kinematics fail to capture such multi-physics behaviors. This can be mitigated by relying on multi-physics simulations enabling impedance control of robot per material parameters like weight, density of material etc., in addition to inverse kinematic simulations. Additionally, integrating multi-modal feedback sensors (vision, haptic, acoustic) and machine learning-based object detection/classification algorithms can enable autonomous course correction in the event of a potential anomaly or collision. The ability to record hand-guided motion, showcased in the pilot (Section 2.4), holds the potential to facilitate telerobotic operation through digital twins of the robot.

While accessing sophisticated and energy-intensive manufacturing machinery, larger robots, and a variety of end-effectors is feasible for terrestrial applications, the same may not apply to extra-terrestrial scenarios like Lunar Construction. It would be logical to categorize recommendations based on the robotic construction of Class I (pre-fabricated Earth-manufactured ready-to-deploy structures carried as payloads in rockets), Class II (pre-fabricated Earth-manufactured modular systems carried as payloads in rockets requiring robotic assembly on-site), and Class III (manufactured components using in-situ lunar resources, subsequently assembled using robotic equipment) infrastructures in extra-terrestrial environments (Mueller, 2022). In addition to researching and developing innovative in-space manufacturing techniques like electro-static additive manufacturing, electron beam melting, sintering, and so on (Ellery, 2021), more emphasis is needed on high-precision in-space manufacturing of large-scale construction components. Until achieving high TRL in-space manufacturing maturity, innovative and optimized DfMA strategies are essential for Class I and II lunar infrastructure. These strategies should aim to optimize construction components for specific objectives like minimizing payload mass, maximizing adaptability for handling by a range of robotic end-effectors (or minimizing exclusivity for handling by a single end-effector), and maximizing high-precision manufacturability using various techniques.

While this pilot study exploring the robotic assembly of the prototype wall system shows moderate success in integrating components, its overall effectiveness is contingent on evaluating the structure's performance. The hygrothermal insulation's efficiency in creating a thermally insulated enclosure relies heavily on a tight seal on all sides. It is evident that some DfMA strategies, such as the use of mortise and tenon joinery, and shaving the sides of the studs, negatively impacted the

shear strength of the prototype, resulting in a loose fit between the rigid foam insulation and structural studs. Future studies should avoid such stop-gap measures, and instead emphasize on real-world applications with actual constraints. Notably, specialized construction needs, like lunar landing and launch pads and pressurized habitats, necessitate extensive air and water filtration/circulation components for functions such as thermal stress management and habitation. Implementing DfMA strategies for seamless robotic assembly is insufficient in these cases; instead, there is a need to develop robotic solutions ensuring quality installation to prevent leaks or anomalies that could adversely affect performance. Overall, to fully leverage robotics for systems integration in both terrestrial and extra-terrestrial infrastructure, conducting robust field demonstrations of complex multi-system, multi-material, multi-trade building assemblies using diverse robotic solutions, followed by subsequent performance testing to validate the effectiveness of the assembled systems is essential (Figure 15).

Figure 15: [Left] Ongoing research simulating robotics for terrestrial building systems integration at NREL (Muthumanickam et al., 2022); [Right] Recent robotics for lunar construction demonstration by GITAI (Nakanose et al., 2023).

4. CONCLUSION

In summary, this pilot study has helped uncover the specific DfMA implementations necessary for robotic assembly of a prototype wall with structural, hygrothermal and rigid electrical components. The goal of the paper was not to propose an all-encompassing solution to robotics for systems integration or outfitting of buildings, instead set the stage for exploring robotics for integration of more complex building systems by highlighting key issues. Lessons learned from this study can help augment robotic construction techniques like additive concrete construction with additional capabilities to install components like reinforcements, thermal barriers, mechanical, electrical, and plumbing systems, thereby leading to fully functional buildings.

5. REFERENCES

3Dnatives. (2021). COBOD printer used for India's first 2-story 3D printed building. 3Dnatives. https://www.3dnatives.com/en/cobod-printer-used-for-indias-first-2-story-3d-printed-building-180120216/

3D Printing Industry. (2023). Indian Army unveils its first two-storey disaster-resilient dwelling unit. 3D Printing Industry. https://3dprintingindustry.com/news/indian-army-unveils-its-first-two-storey-disaster-resilient-dwelling-unit-220076/

Aristidou, A., & Lasenby, J. (2009). Inverse kinematics: a review of existing techniques and introduction of a new fast iterative solver.

Bademosi, F., & Issa, R. R. (2021). Factors influencing adoption and integration of construction robotics and automation technology in the US. Journal of Construction Engineering and Management, 147(8), 04021075.

Bock, T. (2007). Construction robotics. Autonomous Robots, 22, 201-209.

Ellery, A. (2021). Leveraging in situ resources for Lunar Base Construction. Canadian Journal of Civil Engineering, 49(5), 657–674. https://doi.org/10.1139/cjce-2021-0098

Gharbia, M., Chang-Richards, A., Lu, Y., Zhong, R. Y., & Li, H. (2020). Robotic technologies for on-site building construction: A systematic review. Journal of Building Engineering, 32, 101584.

Gusmao Brissi, S., Wong Chong, O., Debs, L., & Zhang, J. (2022). A review on the interactions of robotic systems and lean principles in offsite construction. Engineering, Construction and Architectural Management, 29(1), 383-406.

International Organization for Standardization. (2015). ISO 9001:2015 Quality management systems — Requirements.

International Organization for Standardization. (2016). ISO 14405-1:2016 Geometrical product specifications (GPS) — Dimensional tolerancing — Part 1: Linear sizes.

Melenbrink, N., Werfel, J., & Menges, A. (2020). On-site autonomous construction robots: Towards unsupervised building. Automation in construction, 119, 103312.

Mueller, R. P. (2022). Lunar Base Construction Overview. In ASCE Earth & Space Conference.

Muthumanickam, N.K., Duarte, J.P., Nazarian, S., Bilén, S. G., & Memari, A. (2020). BIM for Design Generation, Analysis, Optimization, and Construction Simulation of a Martian Habitat. In Earth and Space 2021 (pp. 1208-1219).

Muthumanickam, N. K., Duarte, J. P., Nazarian, S., Memari, A., & Bilén, S. G. (2021a). Combining AI and BIM in the design and construction of a Mars habitat. In The Routledge Companion to Artificial Intelligence in Architecture (pp. 251-279). Routledge.

Muthumanickam, N. K. (2021b). Multidisciplinary Design Optimization Framework for Multi-Phase Building Design Process-Technology Demonstration Using Design of Office Building and Robotically 3D Printed Habitat (Doctoral dissertation, Pennsylvania State University).

Muthumanickam, N.K. (2022), "Industrialized and Robotic Construction Advances in Terrestrial Construction and Opportunities in Space Construction", NASA Marshall Space Flight Center Tech Talk 2022. Invited tech talk. July 21, 2022. Virtual. https://www.osti.gov/biblio/1880799-industrialized-robotic-construction-advances-terrestrial-construction-opportunities-space-construction

Nakanose, S., & Nakamura-Messenger, K. (2023). GITAI USA: Providing Safe and Affordable Means of Labor in Space. In ASCEND 2023 (p. 4744).

National Renewable Energy Laboratory, (2022). Industrialized Construction Innovation at NREL [Graphic]. National Renewable Energy Laboratory, Golden, CO, United States. https://www.nrel.gov/buildings/industrialized-construction.html

NPR. (2023). 3D-printed homes level up with a 2-story house in Houston. NPR. https://www.npr.org/2023/01/16/1148943607/3d-printed-homes-level-up-with-a-2-story-house-in-houston

Pan, W., Iturralde, K., Hu, R., Linner, T., & Bock, T. (2020). Adopting Off-site Manufacturing, and Automation and Robotics Technologies in Energy-efficient Building. In ISARC. Proceedings of the International Symposium on Automation and Robotics in Construction (Vol. 37, pp. 1549-1555). IAARC Publications.

Pless, S., Podder, A., Kaufman, Z., Klammer, N., Dennehy, C., Muthumanickam, N. K., ... & Blazek, C. (2022). The Energy in Modular (EMOD) Buildings Method: A Guide to Energy-Efficient Design for Industrialized Construction of Modular Buildings (No. NREL/TP-5500-82447). National Renewable Energy Lab.(NREL), Golden, CO (United States).

M. Tehrani, B., BuHamdan, S., & Alwisy, A. (2023). Robotics in assembly-based industrialized construction: A narrative review and a look forward. International Journal of Intelligent Robotics and Applications, 7(3), 556-574.

Universal Robots. (2023). UR5e [Render]. Universal Robots, Odense S, Denmark. https://www.universal-robots.com/products/ur5-robot/

Universal Robots. (2024). GitHub – Universal Robots/ Universal Robots External Control URCap: Example implementation of how to use ROS driver on-demand in a URCap. GitHub. https://github.com/UniversalRobots/Universal_Robots_ExternalControl_URCap

Xiao, B., Chen, C., & Yin, X. (2022). Recent advancements of robotics in construction. Automation in Construction, 144, 104591.